

Controlling of the polymorphic phase transition on lead-free piezoelectric $\text{Li}_{0.08}(\text{Na}_{0.52+x}\text{K}_{0.48})_{0.92}\text{NbO}_3$ ceramics

Xiao-Kun Zhao, Bo-Ping Zhang*, Lei Zhao, Li-Feng Zhu, Peng-Fei Zhou, Yan Li

School of Materials Science and Engineering, University of Science and Technology Beijing, Xueyuan Road, Haidian Zone, Beijing 100083, China

Received 29 October 2012; received in revised form 15 November 2012; accepted 15 November 2012

Available online 28 November 2012

Abstract

The polymorphic phase transition (PPT) from tetragonal to orthorhombic symmetry was tailored in lead-free piezoelectric ceramics $\text{Li}_{0.08}(\text{Na}_{0.52+x}\text{K}_{0.48})_{0.92}\text{NbO}_3$ ($\text{LN}_{0.52+x}\text{KN}$) by controlling excess Na content, which is opposite to the usually reported orthorhombic–tetragonal phase transition. The grain growth was accelerated by adding excess Na, resulting in an increased grain size from 2–3 μm to 7–8 μm and a bimodal grain size distribution for samples $x=0.015$ –0.04. The optimized piezoelectric properties with, i.e. $d_{33}=226$ pC/N and $k_p=36.8\%$ were obtained in sample $x=0.04$ due to the PPT effect. The corresponding T_C , P_r , and E_r were 468 $^\circ\text{C}$, 25.5 $\mu\text{C}/\text{cm}^2$ and 1.20 kV/mm, respectively.

© 2012 Elsevier Ltd and Techna Group S.r.l. All rights reserved.

Keywords: B. Microstructure; C. Piezoelectric properties; Polymorphic phase transition

1. Introduction

Recently, (Na, K)NbO₃ (NKN)-based ceramics have received particular attention as a potential candidate for lead-free piezoelectric ceramics since Saito et al. [1] have made the breakthrough. It is well known that the morphotropic phase boundary (MPB) plays an important role in enhancing piezoelectric properties for Pb(Zr, Ti)O₃ (PZT) piezoelectric family which has been extensively used in electron devices [2,3]. Similarly, many studies have found so far that the piezoelectric properties could also be improved considerably by the phase transition existing in the NKN-based ceramics. In contrast to the MPB effect separating rhombohedral and tetragonal phases in many PZT systems, two different kinds of phase transition existed in NKN based ceramics which were defined as the MPB or the polymorphic phase transition (PPT). The MPB in NKN was reported to two separate orthorhombic phases O_I and O_{II} in the binary NaNbO_3 – KNbO_3 system [4,5] and in the Li-doped NKN [6], or two tetragonal phases at high temperature in the Li and Ta co-doped NKN system [3,7]. These phase transitions were almost

insensitive to temperature similar to the classical MPB. On the other hand, the PPT in NKN based ceramics was confirmed to be attributed to the adjusting of phase transition separating orthorhombic and tetragonal symmetry to the room temperature. Since pure NKN ceramics generally have the polymorphisms including low temperature (< -123 $^\circ\text{C}$) rhombohedral, room temperature orthorhombic, high temperature (200–410 $^\circ\text{C}$) tetragonal as well as cubic (> 410 $^\circ\text{C}$) phases, a PPT could be achieved by doping Li, Ta, Sb etc. or by turning sintering temperature, which is also dependent strongly on the temperature [1,8–11]. The commonly reported PPT showed a phase transition from orthorhombic to tetragonal (O–T) one, but the study on tailoring PPT from tetragonal to orthorhombic (T–O) one has been reported rarely. Nevertheless, either MPB or PPT was strongly sensitive to the composition and contributes to the excellent piezoelectric properties with $d_{33}=200$ –400 pC/N [6–10]. Hence, the main approach to enhance piezoelectric properties was reported to be usually focused on modifying composition and optimizing sintering temperature, in which the latter essentially varied in alkali metals content because of their volatilization during sintering [12–14]. The evaporation of alkali metals became severe at temperatures above 1000 $^\circ\text{C}$, leading to the inferior

*Corresponding author. Tel.: +86 10 62334195.

E-mail address: bpzhang@ustb.edu.cn (B.-P. Zhang).

repeatability of sintering process and the instability of piezoelectric properties [14]. A viable option to avoid the evaporation was to reduce the sintering temperature below 1000 °C, in which sintering aids such as Na₂O, Li₂O, CuO, MgO and ZnO were reported to be effective in decreasing the densification sintering temperature for the NKN-based ceramics [15–19]. Among them Na₂O was effective in facilitating the grain growth, compensating the volatilization of alkali metal and modifying the phase structure [6,16]. In the present study, an attempt on tailoring the PPT from tetragonal to orthorhombic symmetry was carried out in lead-free Li_{0.08}(Na_{0.52+x}K_{0.48})_{0.92}NbO₃ (LN_{0.52+x}KN) piezoelectric ceramics prepared by normal sintering below 1000 °C. The microstructure, phase structure as well as electrical properties were investigated with an emphasis on the influence of excess Na content.

2. Experimental procedures

Sodium carbonate (Na₂CO₃, 99.8%), potassium carbonate (K₂CO₃, 99%), lithium carbonate (Li₂CO₃, 97%), and niobium oxide (Nb₂O₅, 99.99%) were used as raw materials. These materials were mixed with a nominal composition of Li_{0.08}(Na_{0.52+x}K_{0.48})_{0.92}NbO₃ (LN_{0.52+x}KN) ($x=0, 0.015, 0.025, 0.032, 0.04, 0.05, 0.06, \text{ and } 0.08$) by ball milling in an ethanol solution in a planetary ball mill. After ball milling for 4 h, the slurries were dried at 80 °C for 12 h and calcinated at 850 °C for 4 h. The synthesized powders were then compacted to disks of 10 mm in diameter and 1.2 mm in thickness, followed by normal sintering in air at 990 °C for 2 h. The sintered samples were poled under a dc field of 3–4 kV/mm at 120 °C for 15 min in a silicone oil bath.

The density of samples was determined by Archimedes' method. The crystal structures were determined using X-ray powder diffraction with a CuK α radiation ($\lambda=1.5406$ Å) filtered through a Ni foil (Rigaku; RAD-B system, Tokyo, Japan). The microstructure was observed by a scanning electron microscope (SEM, S-450, Hitachi, Tokyo, Japan). The temperature dependence of the dielectric properties was examined using a programmable furnace with an LCR analyzer (TH2828S, Tonghui Electronics, Shenzhen, China) at 1 kHz in the temperature range of 30–550 °C. The piezoelectric constant d_{33} was measured using a quasistatic piezoelectric coefficient testing meter (ZJ-3A, Institute of Acoustics, Chinese Academy of Sciences, Beijing, China). The electromechanical coupling coefficients k_p was determined from the resonance–antiresonance method performed on the basis of IEEE standards using an Agilent 4294A precision impedance analyzer (Hewlett-Packard, Palo Alto, CA). The ferroelectric hysteresis loops were measured at room temperature using a ferroelectric tester (RT6000HVA, Radiant Technologies, Inc., Albuquerque, NM).

3. Results and discussion

Fig. 1 shows the apparent density and relative density of the LN_{0.52+x}KN ceramics sintered at 990 °C as a function

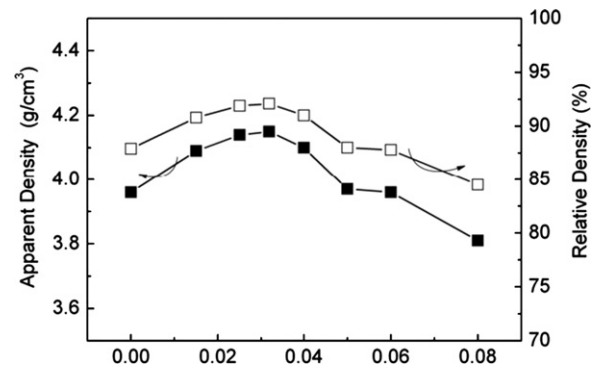


Fig. 1. Apparent density (ρ) and relative density (ρ_r) of LN_{0.52+x}KN ceramics.

of the excess Na content (x), in which the theoretical density is 4.51 g/cm³. Both the apparent density and relative density increase with raising x from 0 to 0.032, and reach the peak values of 4.15 g/cm³ and 92.1% in sample $x=0.032$, respectively. Generally, the sintering temperature should be higher than 1040 °C to synthesize a dense LNKN bulk with a relative density more than 90% [8]. Although the densification sintering temperature could be lowered below 1000 °C by adding sintering aids such as CuO, MgO and ZnO, the piezoelectric properties dropped simultaneously [14,15,18,19]. In this work, a relative density above 90% was obtained for samples sintered even at 990 °C by adding excess Na without any other sintering aid, suggesting the good sintering activity of the component Na.

Fig. 2 shows the SEM images of the fractured surface for the LN_{0.52+x}KN ceramics sintered at 990 °C. All the ceramics show square or rectangular grains, in which a faceted interface is observed in some grains as shown in the inset of Fig. 1(a). The grain of the sample $x=0$ shows a relatively homogeneous size distribution of 2–3 μm and grows by adding excess Na. A bimodal grain size distribution is observed for samples $x=0.015$ –0.04 in Fig. 2(b–d). Further adding of excess Na to $x=0.06$ and 0.08 induced a homogeneous structure with a constant grain size of about 7–8 μm . The grown microstructure may be due to the lowered critical driving force for rapid grain growth by adding excess Na [16]. However, the grain growth rate varied for the grains with different morphologies even for the same sample [16]. The abnormal grain growth occurred when the interfaces or boundaries were faceted, while normal grain growth occurred only in systems with rounded interfaces or boundaries [16,20]. As a result, the bimodal grain size distribution is formed in Fig. 2(b–d). Further increasing Na content reduces the critical driving force of most grains and produces their growth as well as the homogenization of the grains in Fig. 2(e–f). The small grains occupy the pores between the large grains due to the bimodal grain size distribution and brings about a high density for samples $x=0.015$ –0.04, which corresponds to the changes of density shown in Fig. 1.

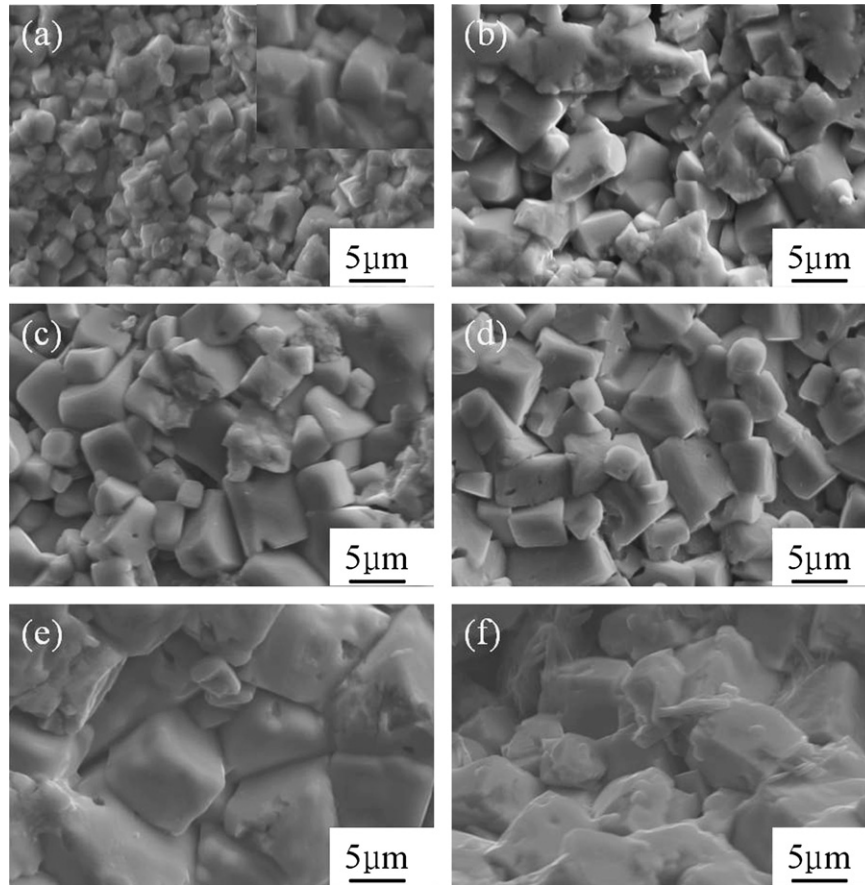


Fig. 2. SEM images of the fractured surface for the LN_{0.52+x}KN ceramics: (a) $x=0$, (b) $x=0.015$, (c) $x=0.025$, (d) $x=0.04$, (e) $x=0.06$, and (f) $x=0.08$.

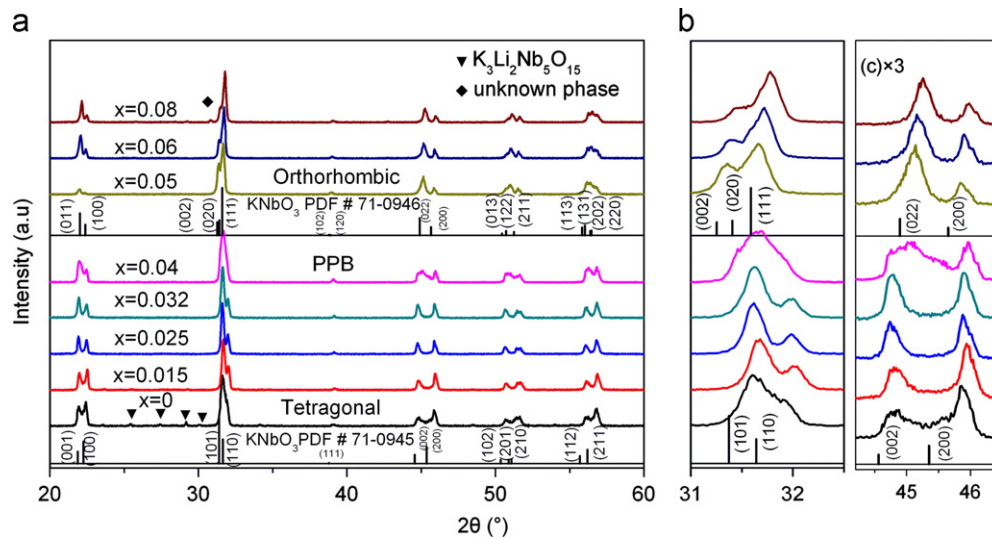


Fig. 3. X-ray diffraction patterns of the LN_{0.52+x}KN ceramics.

Fig. 3 shows the X-ray diffraction patterns for the LN_{0.52+x}KN ceramics sintered at 990 °C, in which the main phase has a perovskite structure. The diffraction peaks cited from the tetragonal (T) KNbO₃ (PDF#71-0945) and the orthorhombic (O) one (PDF#71-0946) are indicated

by vertical lines for comparison, in which the ratios of two diffraction peaks around 45° are obviously different as shown in the enlarged XRD patterns of angles ranged from 44° to 46° in Fig. 3(c). The former ratio of (002)_T to (200)_T is less than 1, while the later ratio of (022)_O and (200)_O is greater

than 1. Hence, the main phase for samples $x=0-0.032$ and $x=0.04-0.08$ possesses tetragonal and orthorhombic symmetry, respectively. A PPT from tetragonal symmetry to orthorhombic one appears in the composition $x=0.04$. This tetragonal–orthorhombic (T–O) transition is opposite to the orthorhombic–tetragonal (O–T) phase transition which was generally reported in a lot of Li-doped NKN based ceramics [3,8,12,14]. The present T–O transition is due to the actually decreased Li content by raising x , which suggests the controllable phase structure. A second phase $K_3Li_2Nb_5O_{15}$ (ICDD 52-0157) with a tetragonal tungsten bronze structure appears in the sample $x=0$, which was usually found in Li, Ta, Sb doped or co-doped NKN based ceramics with a high Li content [7,9] and was adverse to the piezoelectric properties. Our result suggests that adding excess Na content is effective to suppress the formation of $K_3Li_2Nb_5O_{15}$ and to form a single phase in the samples $0.025 < x < 0.06$. However, further adding excess Na content to 0.08 leads to forming an unknown phase, which may be a kind of Na-rich phase due to the solid solution limitation of Na in the A site of ABO_3 structure.

Fig. 4 shows the variation of the unit-cell parameters for the main phase as a function of x , which were calculated from the corresponding XRD patterns of the $LN_{0.52+x}KN$ ceramics. The samples reveal a tetragonal symmetry with the parameters $a=b < c$ for samples $x=0-0.032$ and an orthorhombic one with parameters $a < b < c$ for samples $x=0.05-0.08$. The volume of unit-cell in Fig. 4(b)

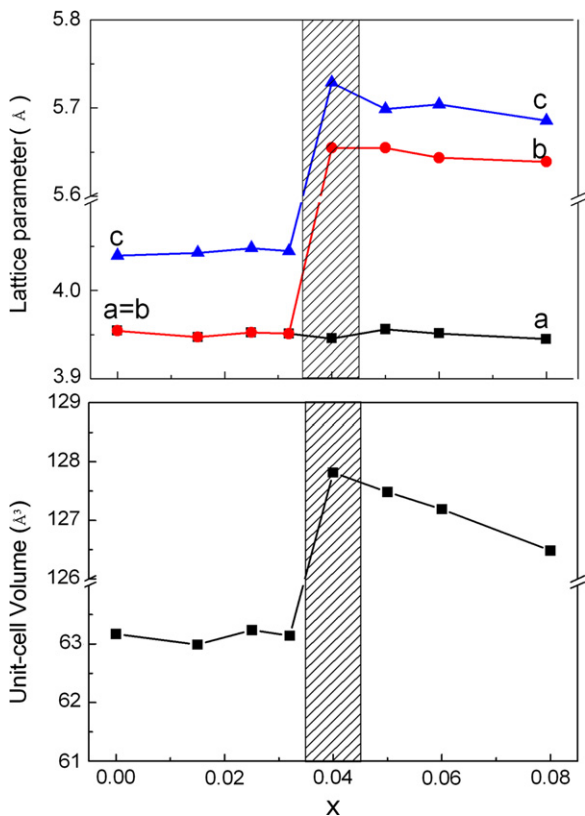


Fig. 4. Lattice parameters of $LN_{0.52+x}KN$ ceramics.

maintains at the range of 62.99 \AA^3 to 63.14 \AA^3 by adding Na from $x=0$ to $x=0.032$ and then shrinks from 127.81 \AA^3 to 126.48 \AA^3 as increasing x to 0.08 in the orthorhombic region. The shrinkage of the unit-cell indicates that the excess Na^+ has diffused into the lattices since the smaller ionic radius of Na^+ (0.97 \AA) than that of K^+ (1.33 \AA), which is also supported by the X-ray diffraction patterns in Fig. 3(b, c), in which the 2θ diffraction peaks of (002), (020), (111) (022), and (200) shifts to a higher angle for samples $x=0.05-0.08$ and reveals the decrement of the corresponding space distance.

Fig. 5 shows the piezoelectric properties of poled $LN_{0.52+x}KN$ ceramics as a function of x . The piezoelectric coefficient (d_{33}) and planar mode electromechanical coupling coefficient (k_p) for sample $x=0$ are 40 pC/N and 12.3% respectively. The poor piezoelectric properties are attributed to the appearance of the second phase $K_3Li_2Nb_5O_{15}$ as shown in Fig. 3. Both d_{33} and k_p increase with addition of excess Na, showing the peak values of 226 pC/N and 36.7% for sample $x=0.04$, and then decrease to 115 pC/N and 24.1% by further increasing x to 0.08. The optimized piezoelectric properties for sample $x=0.04$ are due to the PPT behavior separating tetragonal and orthorhombic

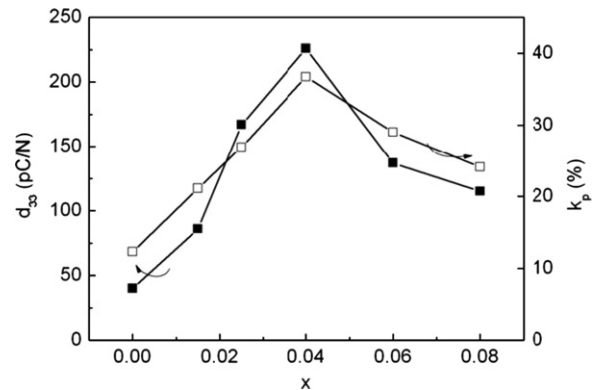


Fig. 5. Piezoelectric coefficient and planar mode electromechanical coupling coefficient for the $LN_{0.52+x}KN$ ceramics.

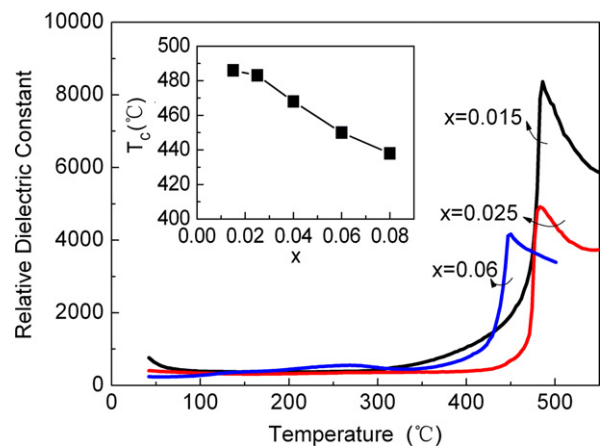


Fig. 6. Temperature dependence of relative dielectric constant ϵ_r and the Curie temperatures for $LN_{0.52+x}KN$ ceramics.

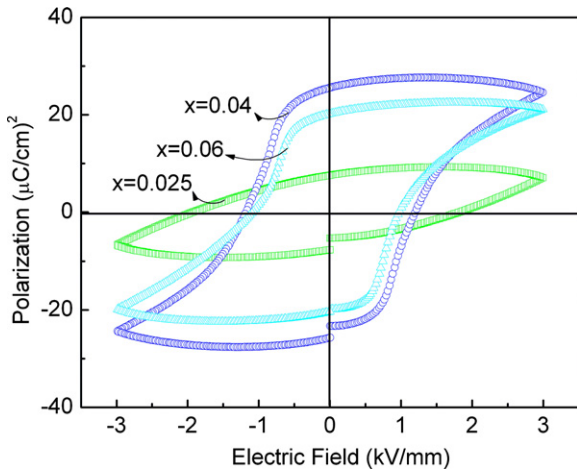


Fig. 7. Polarization hysteresis loops of the $\text{LN}_{0.52+x}\text{KN}$ ceramics with $x=0.025, 0.04,$ and 0.06 .

phase along with the absence of any other second phase.

Fig. 6 shows the temperature dependence of relative permittivity ϵ_r and the Curie temperature T_C for the $\text{LN}_{0.52+x}\text{KN}$ ceramics, which were measured at 1 kHz. The T_C of sample $x=0.015$ is 486°C which is attributed to the high Li content of 8 mol%. The T_C was shifted slightly to a lower temperature by raising Na content, which can be interpreted as a result of actually reduced Li content [7]. On the other hand, the T_C for the sample $x=0.04$ owning the peak value of d_{33} 226 pC/N maintains at 460°C in spite of the slightly decreased trend, which is much higher than 253°C in the Li, Ta and Sb co-doped samples [1].

Fig. 7 shows the polarization hysteresis curves for the $\text{LN}_{0.52+x}\text{KN}$ ceramics. All the samples have a saturation hysteresis loops, showing promising ferroelectric properties. For samples $x=0.025, 0.04,$ and 0.06 , the remanent polarization (P_r) values are 7.53, 25.5, and $20.2\ \mu\text{C}/\text{cm}^2$, while the corresponding coercive fields (E_C) are 1.83, 1.20, $0.97\ \text{kV}/\text{mm}$, respectively. The peak P_r value for sample $x=0.04$ is due to the more spontaneous polarization directions in the PPT composition coexisting tetragonal–orthorhombic ferroelectric phases [3]. The decreased E_C is due to the decreased grain boundary resulted from the grain growth which prevents the polarization in the ceramics [21].

4. Conclusions

In this work, $\text{Li}_{0.08}(\text{Na}_{0.52+x}\text{K}_{0.48})_{0.92}\text{NbO}_3$ ceramics were prepared by normal sintering at 990°C . A PPT from tetragonal to orthorhombic symmetry with increasing excess Na content appeared in the sample $x=0.04$, which was opposite to the generally reported the orthorhombic–tetragonal phase transition. The grain growth was accelerated by adding excess Na, bringing about grown grains and a bimodal grain size distribution for samples $x=0.015$ – 0.04 . The d_{33} and k_p reached the peak values

226 pC/N and 36.8% due to PPT effect, respectively. The T_C maintained at 468°C for sample $x=0.04$ and decreased with increasing Na content. The corresponding P_r and E_C were $25.5\ \mu\text{C}/\text{cm}^2$ and $1.2\ \text{kV}/\text{mm}$, respectively. The controllable PPT behavior is convenient for enhancing the piezoelectric properties in the lead-free NKN based ceramics.

Acknowledgments

This work was financially supported by Specialized Research Fund for the Doctoral Program of Higher Education (Grant no. 20090006110010).

References

- [1] Y. Saito, H. Takao, T. Tani, T. Nonoyama, K. Takatori, T. Homma, T. Nagaya, M. Nakamura, Lead-free piezoceramics, *Nature* 432 (2004) 84–87.
- [2] B. Jaffe, W.R. Cook Jr., H. Jaffe, in: *Piezoelectric Ceramics*, Academic Press, New York, 1971.
- [3] J. Rödel, W. Jo, K.T.P. Seifert, E.M. Anton, T. Granzow, D. Damjanovic, Perspective on the development of lead-free piezoceramics, *Journal of the American Ceramic Society* 92 (2009) 1153–1177.
- [4] B.P. Zhang, J.F. Li, K. Wang, H.L. Zhang, Compositional dependence of piezoelectric properties in $\text{Na}_x\text{K}_{1-x}\text{NbO}_3$ lead-free ceramics prepared by spark plasma sintering, *Journal of the American Ceramic Society* 89 (2006) 1605–1609.
- [5] Y.J. Dai, X.W. Zhang, K.P. Chen, Morphotropic phase boundary and electrical properties of $\text{K}_{1-x}\text{Na}_x\text{NbO}_3$ lead-free ceramics, *Applied Physics Letters* 94 (2009) 042905.
- [6] H.T. Li, B.P. Zhang, P.P. Shang, Y. Fan, Q. Zhang, Phase transition and high piezoelectric properties of $\text{Li}_{0.058}(\text{Na}_{0.52+x}\text{K}_{0.48})_{0.942}\text{NbO}_3$ lead-free Ceramics, *Journal of the American Ceramic Society* 94 (2011) 628–632.
- [7] J.J. Zhou, J.F. Li, K. Wang, X.W. Zhang, Phase structure and electrical properties of (Li, Ta)-doped (K, Na) NbO_3 lead-free piezoceramics in the vicinity of $\text{Na}/\text{K}=50/50$, *Journal of Materials Science* 46 (2011) 5111–5116.
- [8] Y.P. Guo, K. Kakimoto, H. Ohsato, Phase transitional behavior and piezoelectric properties of $\text{Na}_{0.5}\text{K}_{0.5}\text{NbO}_3$ – LiNbO_3 ceramics, *Applied Physics Letters* 85 (2004) 4121–4123.
- [9] S.J. Zhang, R. Xia, T.R. Shrout, G.Z. Zang, J.F. Wang, Piezoelectric properties in perovskite $0.948(\text{K}_{0.5}\text{Na}_{0.5})\text{NbO}_3$ – 0.052LiSbO_3 lead free ceramics, *Journal of Applied Physics* 100 (2006) 104108.
- [10] Y.P. Guo, K. Kakimoto, H. Ohsato, $\text{Na}_{0.5}\text{K}_{0.5}\text{NbO}_3$ – LiTaO_3 lead-free piezoelectric ceramics, *Materials Letters* 59 (2005) 241–244.
- [11] H.J. Trodahl, N. Klein, D. Damjanovic, N. Setter, B. Ludbrook, D. Rytz, M. Kuball, Raman spectroscopy of (K, Na) NbO_3 and (K, Na) $_{1-x}\text{Li}_x\text{NbO}_3$, *Applied Physics Letters* 93 (2008) 262901.
- [12] P. Zhao, B.P. Zhang, J.F. Li, High piezoelectric d_{33} coefficient in Li-modified lead-free (Na, K) NbO_3 ceramics sintered at optimal temperature, *Applied Physics Letters* 90 (2007) 242909.
- [13] P. Zhao, B.P. Zhang, J.F. Li, Enhanced dielectric and piezoelectric properties in LiTaO_3 -doped lead-free (K, Na) NbO_3 ceramics by optimizing sintering temperature, *Scripta Materialia* 58 (2008) 429–432.
- [14] K. Wang, J.F. Li, (K, Na) NbO_3 -based lead-free piezoceramics: phase transition, sintering and property enhancement, *Journal of Advanced Ceramics* 1 (2012) 24–37.
- [15] H.Y. Park, C.W. Ahn, K.H. Cho, S. Nahmw, Low-temperature sintering and piezoelectric properties of CuO-added $0.95(\text{Na}_{0.5}\text{K}_{0.5})$

- $\text{NbO}_3\text{-}0.05\text{BaTiO}_3$ Ceramics, *Journal of the American Ceramic Society* 90 (12) (2007) 4066–4069.
- [16] M.S. Kim, D.S. Lee, E.C. Park, Effect of Na_2O additions on the sinterability and piezoelectric properties of lead-free $95(\text{Na}_{0.5}\text{K}_{0.5})\text{NbO}_3\text{-}5\text{LiTaO}_3$ Ceramics, *Journal of the European Ceramic Society* 27 (2007) 4121–4124.
- [17] M.S. Kim, S.J. Jeong, J.S. Song, Microstructures and piezoelectric properties in the Li_2O -excess $0.95(\text{Na}_{0.5}\text{K}_{0.5})\text{NbO}_3\text{-}0.05\text{LiTaO}_3$ Ceramics, *Journal of the American Ceramic Society* 90 (2007) 3338–3340.
- [18] H.T. Li, B.P. Zhang, Q. Zhang, P.P. Shang, G.L. Zhao, Microstructure, crystalline phase and electrical properties of $\text{Li}_{0.06}(\text{Na}_{0.5}\text{K}_{0.5})_{0.94}\text{Nb}_{(1-2x/5)}\text{Mg}_x\text{O}_3$ lead-free piezoelectric ceramics, *International Journal of Minerals and Materials* 17 (2010) 340–346.
- [19] H.T. Li, B.P. Zhang, M. Cui, W.G. Yang, N. Ma, J.F. Li, Microstructure, crystalline phase, and electrical properties of ZnO-added $\text{Li}_{0.06}(\text{Na}_{0.535}\text{K}_{0.48})_{0.94}\text{NbO}_3$ ceramics, *Current Applied Physics* 11 (2011) S184–S188.
- [20] B.K. Lee, S.Y. Cuang, S.J. Kang, Grain boundary faceting and abnormal grain growth in BaTiO_3 , *Acta Materialia* 48 (2000) 1575–1580.
- [21] Q.R. Yin, B.H. Zhu, in: *Microstructure, Property and Processing of Functional Ceramics*, Metallurgical Industry Press, Beijing, 2005.